D34

N85-16923

CHALLENGES IN THE DEVELOPMENT OF THE ORBITER ACTIVE THERMAL CONTROL SUBSYSTEM

Author:

John R. Nason
Senior Analytical Engineer
United Technologies Corporation
Hamilton Standard Division
Windsor Locks, Connecticut

Contributing Authors:

Frederic A. Wierum
Professor of Mechanical and Aerospace Engineering
Rice University
Houston, Texas

James L. Yanosy
Analytical Engineer
United Technologies Corporation
Hamilton Standard Division
Windsor Locks, Connecticut

ABSTRACT

A number of major challenges were faced in the design and development of the Orbiter Active Thermal Control Subsystem (ATCS). At the system level, the initial challenges were to define an approach that would interface dual Freon coolant loops with multiple coolant loops from other vehicle subsystems with the lowest weight penalty to the Orbiter; and to provide highly responsive vehicle heat rejection throughout all of the Orbiter mission phases.

Optimized heat exchangers, representing an advance in the state-of-the-art in heat exchanger design, were developed to transfer heat between the orbiter Freon coolant loops and five other vehicle systems. The heat exchangers interface four or five separate coolant loops in a single unit while maximizing performance and minimizing weight, volume and coolant loop pumping power. This paper includes a description of the various heat exchanger configurations, optimization techniques used in their design and performance characteristics realized during testing and flight operations.

Flash evaporation was selected as a highly efficient and responsive means for cooling the Orbiter Freon loops during ascent and entry. It also provides supplemental cooling on-orbit. The Flash Evaporator Subsystem (FES) utilizes cyclic water spray cooling in a chamber maintained at or below the water triple point pressure. Because of the dynamic nature of the flash evaporation process, challenges were faced in hardware and control scheme development and in performance verification testing of the subsystem under flight simulated conditions. This paper includes a summary of the basic heat transfer research conducted by Rice University to identify the fundamental heat transfer processes involved in water spray cooling in support of the FES design. Also included is a discussion of the high fidelity dynamic analytical model of the FES that was generated to aid in the design of control logic, evaluate performance and simulate ground test and flight anomalies. A description of the FES and Integrated ATCS testing conducted in the SESL chamber A at NASA-JSC is also presented.

NOMENCLATURE

$M_f(i)$	=	mass of Freon in core wall segment "i", lbm
C_{pf}	=	specific heat of Freon, Btu/lbm-^{0}F
$\bar{T}_f(i)$	=	average temperature of Freon in core segment "i", ^{0}F
t	=	time, sec
$\dot{m}_f$	=	Freon flow, lbm/sec
$T_{fin}(i)$	=	inlet Freon temperature at segment "i", ^{0}F
$T_{fout}(i)$	=	exit Freon temperature at segment "i", ^{0}F
h_f	=	Freon film coefficient, Btu/hr-ft^2-^{0}F
$A(i)$	=	heat transfer area between Freon and core wall, ft^2
$T_w(i)$	=	wall temperature of core segment "i", ^{0}F
$M_w(i)$	=	mass of core wall segment "i", lbm
C_{pw}	=	specific heat of core wall metal, Btu/lbm-^{0}F
C	=	conductance between core wall segments, Btu/hr-^{0}F
$T_w(i-1)$	=	wall temperature of core segment "i-1", ^{0}F
$T_w(i+1)$	=	wall temperature of core segment "i+1", ^{0}F
$Q_e(i)$	=	heat loss from wall segment "i" to evaporate water, Btu/hr
β	=	water spray angle
$f(\beta)$	=	cumulative mass of water sprayed into core up to angle β as a fraction of the total
ϕ	=	curve fit constant equal to the water spray angle at $f(\beta) = 0.5$
m	=	curve fit constant equal to the slope of $f(\beta)$ at $f(\beta) = 0.5$

INTRODUCTION

Because the nature of the Space Shuttle mission is different from previous spacecraft, new challenges were faced in the design and development of the Orbiter Active Thermal Control Subsystem (ATCS). Hardware weight and volume have always been of paramount concern in spacecraft design. However, they take on added importance for the orbiter since it is reusable and every pound of hardware weight must be launched to low earth orbit a maximum of 100 times during the life of the vehicle. Economics also had a stronger influence on the orbiter hardware design than on previous spacecraft. Every pound of orbiter equipment displaces a pound of payload and the revenue that could be realized from that payload.

Reliability, ground maintenance and turn-around time also were strong considerations in the system design phase. In order to provide an economically viable Space Transportation System, the Shuttle must be kept flying with a maintenance philosophy approaching that of a commercial airline.

These design drivers made it doubly important to optimize the ATCS from a performance, weight and volume standpoint, while providing sufficient redundancy and flexibility to accommodate failures during flight without adversely affecting the mission or ground turn-around time.

Extensive system engineering optimization studies, a basic research program, sophisticated dynamic computer analyses and extraordinary testing were used to meet the ATCS challenges.

Both system and component level challenges were encountered during the design and development phases of the Shuttle ATCS program. Some of the most challenging areas are discussed in the following sections.

SYSTEM DEFINITION

Providing the desired flexibility at minimum weight and volume was the biggest challenge at the system level. The ATCS performs the following three basic functions:

- Cools or heats other subsystems through interface heat exchangers.
- Transports heat from sources to sinks by means of dual Freon coolant loops.
- Rejects heat by various means dependent on mission phase.

A functional block diagram of the subsystem is shown in Figure 1.

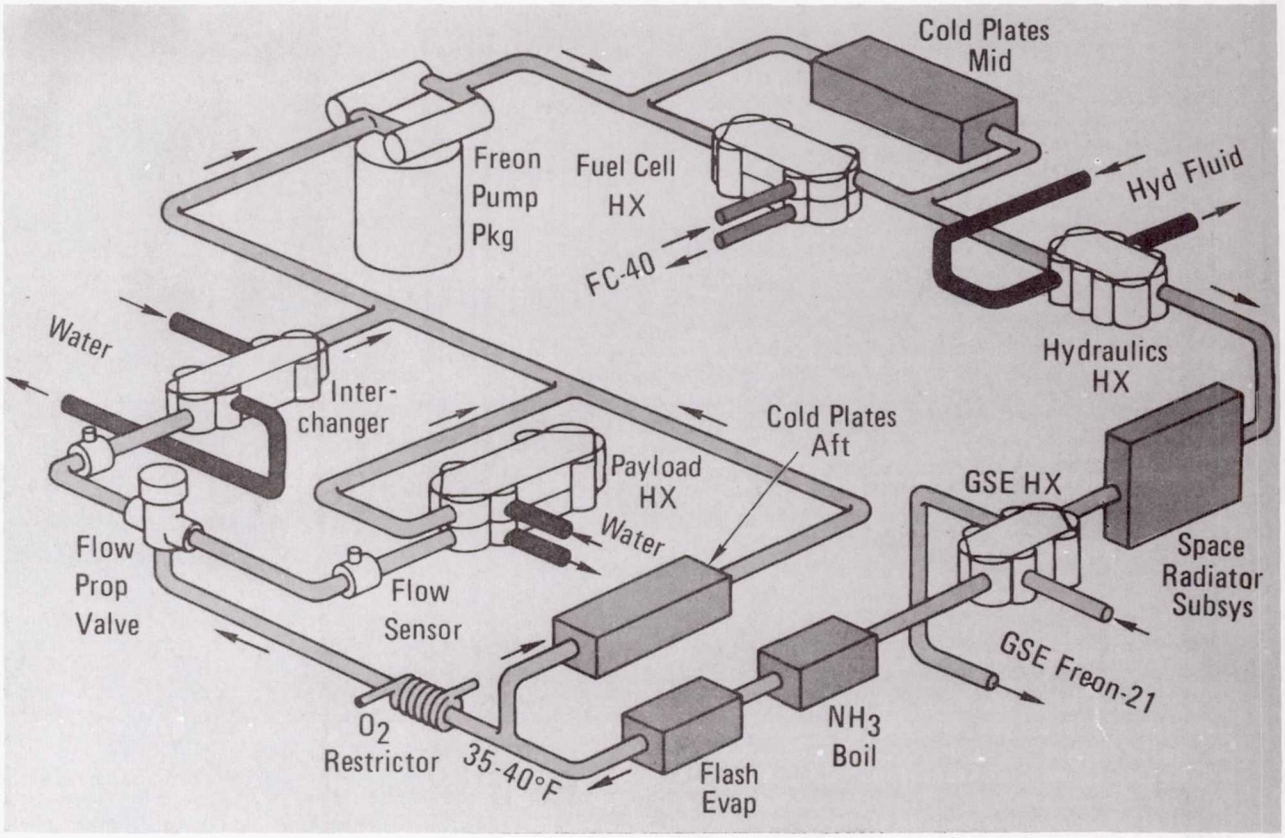

FIGURE 1 FREON COOLANT LOOP SCHEMATIC

Other equipment cooled or heated by the ATCS includes:

- o Cabin Atmosphere Revitalization Subsystem - two redundant water coolant loops.
- o Fuel Cell Power Systems - three separate FC-40 coolant loops.
- o Payloads - two separate payload coolant loops using either Freon or water.
- o Hydraulic Systems - three separate hydraulic fluid loops.
- o Cold Plate mounted electronic equipment.

(Only one each of the interfacing coolant loops is shown in Figure 1.)

Heat transport from heat sources to heat sinks is provided by dual Freon-21 coolant loops (only one loop is shown in Figure 1). Extensive trade-off studies were performed during the shuttle definition phase to arrive at the optimum mode of operation. The mode selected was that of operating both Freon loops normally with single loop operation only in a failure mode providing on-line redundancy rather than standby redundancy. This approach saved considerable fixed weight and power over an approach where a single loop provides total cooling during normal operation with the second redundant loop on standby. The dual loop approach does require redundant pumps in each loop and a reduction in heat load (power usage) from normal when only one loop is operating. This, however, was deemed acceptable in a failure case and does not adversely affect the safety of the crew and vehicle.

Heat rejection must be provided during a number of vastly different mission phases by different means. Trade-off studies during the shuttle definition phase resulted in the need for four different heat sink devices to provide heat rejection during all of the mission phases. The major mission phases and the type of heat rejection provided are:

- o Prelaunch/Postlanding - ground support equipment cooling
- o Launch - thermal inertia
- o Ascent/Entry - water evaporation
- o On-orbit - space radiation with supplemental water evaporation
- o Landing - ammonia evaporation

Prior to launch and at some time after landing, cooling is provided by a ground cart refrigeration system. A trade-off study was conducted that resulted in the use of a permanently installed Ground Support Equipment (GSE) heat exchanger in the orbiter cooling loops to interface with the ground cooling loop. Cold Freon is supplied to the vehicle through fly-away quick disconnects. The high GSE Freon flow and cold temperature minimize heat exchanger size and weight. Although a small weight penalty results because the unit must be carried into orbit every mission, isolation is provided between the vehicle and ground loops resulting in a much safer and more reliable design.

Heat rejection during the on-orbit mission phase is provided by radiation to space. This was an obvious choice over expendable evaporation. If water was used as an evaporant, approximately 16,400 lb would be required for a seven day mission (maximum payload heat load) while the fuel cell would produce only 2400 lb (available for heat rejection). The difference (14,000 lb) would have to be carried to orbit resulting in a tremendous weight penalty.

Water evaporation was the choice, however, for heat rejection following launch until the space radiator is deployed and during entry after the radiator is stowed inside the payload bay doors. These mission phases are relatively short and the launch weight penalty is small. Water is used as the evaporant because it has a latent heat of vaporization double that of any other potential evaporant, and it can be replenished on-orbit by the fuel cells.

The water evaporation pressure (saturation pressure) and corresponding saturation temperature must be maintained at low enough levels (less than 0.1 psia and 35°F) to cool the Freon loops to 40°F. An altitude above approximately 140,000 ft must be reached before the desired ambient pressure is attained. For this reason water is not an acceptable evaporant for launch and landing.

Prior to launch, cooling is provided by ground support equipment. It takes the shuttle slightly over two minutes to reach an altitude where water evaporation becomes effective. There is sufficient thermal inertia in the system to limit the Freon loop temperature rise that active heat rejection is not required for the first two and a half minutes of launch.

An ammonia boiler is used to provide cooling during the last ten minutes of flight and until ground support equipment is connected (about 10 to 15 minutes following landing). This 20 to 25 minute period is too long to rely totally on thermal inertia. Ammonia, although toxic, is the most efficient evaporant with the exception of water, having a latent heat of vaporization about half that of water. But, because of the short time period involved, the quantity of ammonia required is small.

SYSTEM LEVEL CHALLENGES

An integral part of the system level trade-off studies and one of the greatest ATCS challenges was defining an efficient means for interfacing the two Freon coolant loops with the multiple cooling loops from other systems. The result was an innovative heat exchanger design approach that allows heat transfer between four or five separate cooling loops in a single unit. Another major challenge resulting from the system level studies was the design and development of a highly responsive, long life, low maintenance water evaporator that operates over a large range of heat loads with a gravity range from 0g to 3g's. Both of these component challenges are discussed in detail in the following sections.

INTERFACE HEAT EXCHANGERS

Optimization of the Orbiter ATCS required advances in the state-of-the-art of compact heat exchanger design and manufacture. In the areas of fin density, flow configuration and headering, the heat exchanger designs have gone beyond anything previously manufactured for the space program.

The design of these heat transfer devices was approached with a concentrated effort to minimize weight, volume and power impact on the vehicle.

Fin Optimization

Optimization studies concluded that, to a practical limit, the highest density design yields the lightest and smallest unit. A measure of the compactness of a heat exchanger, both from a weight and volume standpoint, is the term (A/V), heat transfer area divided by core volume. This term is plotted against fin height and number of fins per inch (FPI) in Figure 2.[1] Fin heights ranging from 0.010 to 0.200 inches and FPI ranging from 8 to 48 were investigated. The obvious conclusion is that denser fins yield higher values of A/V.

The shorter more dense fins give the added advantages of higher fin efficiency, improving heat transfer performance and the ability to use thinner parting sheets reducing weight. Smaller core sizes also result in smaller, lighter headers, lighter core bands, passage closure bars and mounting feet and less fluid weight.

Prior to the shuttle program, the densest fin configuration successfully manufactured by Hamilton Standard in stainless steel was a fin height of 0.050 in. and 24 FPI. After reviewing manufacturing limitations it was concluded that fin heights as small as 0.020 in. and FPI as high as 32 could be manufactured with some development and this fin configuration was selected for use on the orbiter. They resulted in a 55% improvement in A/V.

In order to size and predict the performance of heat exchangers with the selected fin density, existing fin data for Coburn and friction factors had to be generalized and extrapolated to fin heights 40% less and FPI 33% greater than that for which data was available. A number of manufacturing challenges were also faced. Techniques for manufacturing the dense fin material were refined. New techniques for fixturing and brazing cores were developed. Techniques were also developed to seal minute leaks at closure bars and between layers in order to meet the extremely low leakage rate required by the Orbiter ATCS.

In optimizing a design for a given set of requirements, total equivalent weight including heat exchanger, fluid and power equivalent weight must be considered. Figure 3[1] presents an example of this trade-off for the Interchanger that cools the cabin water loops.

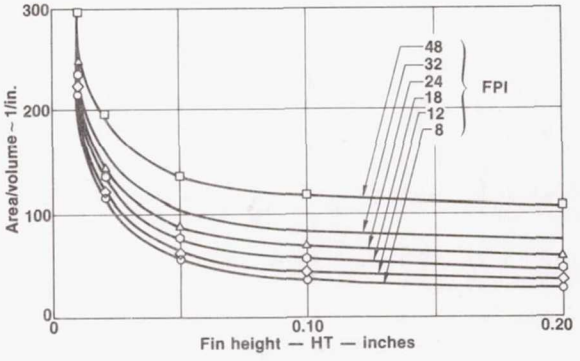

FIGURE 2 FIN OPTIMIZATION

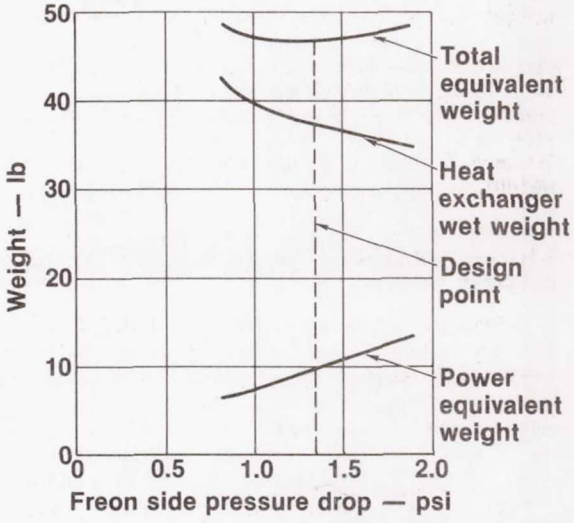

FIGURE 3 INTERCHANGER OPTIMIZATION

In all cases except the Hydraulics heat exchanger the optimum fin configuration was a height of 0.020 inches and 32 FPI. Because of the very viscous hydraulic fluid, that heat exchanger optimized at a fin height of 0.050 inches and 32 FPI.

Configuration Optimization

In each of the five different ATCS applications (coolant loop interfaces), various heat exchanger system configurations or arrangements are possible. Two of the applications will be discussed as examples. Figure 4 shows three of the configurations considered for the Interchanger. Both the 4 two-fluid and 2 three-fluid heat exchanger configurations proved to be heavier in total equivalent weight than the single four-fluid unit. In addition, a single heat exchanger shows a considerable cost advantage over multiple heat exchangers.

Even though one of the ARS water loops is not operating normally, very little performance is lost in the four-fluid heat exchanger because of the way in which the layers are arranged. Figure 5 shows this arrangement. Each active water loop layer has an active Freon loop layer on either

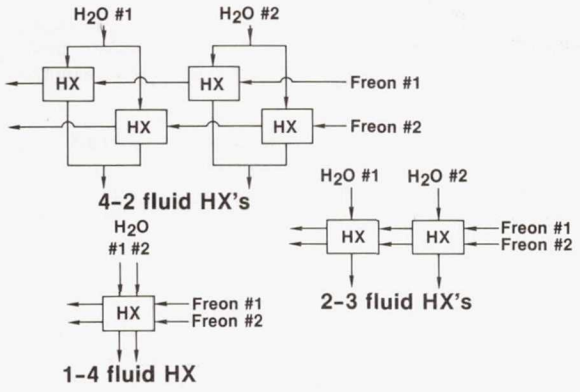

FIGURE 4 INTERCHANGER CANDIDATE APPROACHES

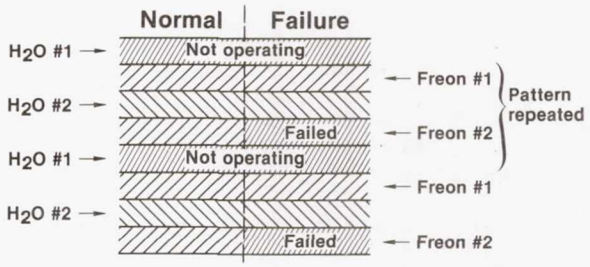

FIGURE 5 INTERCHANGER LAYERS

side resulting in high performance. The only performance difference over a two-fluid heat exchanger is that the effective fin height of the Freon layers is doubled resulting in a slight loss of UA. However, with the short fins the performance degradation is small. In the event one of the two Freon loops fails, each active water layer still has an active Freon layer on one side but must conduct heat through two dead layers on the other side. Again, because of the short fin height the performance degradation is minimal due to a loss of UA.

The second example of a system configuration trade-off is for the fuel cell heat exchanger. In this case, the interfacing of five coolant loops must be accomplished. Figure 6 shows the options considered, a 6 two-fluid, 3 threefluid, and a single five-fluid heat exchanger approach. The single five-fluid unit is actually 2 four-fluid heat exchangers manufactured in a single stack. Trade-off studies showed the single five-fluid heat exchanger to be lightest in total equivalent weight.

A refinement of the selected approach was effected by building up the two heat exchanger cores in a single stack making one unit with appropriate headering. This again shows a cost advantage over multiple units.

A different layer arrangement was required for the fuel cell heat exchanger from that presented for the Interchanger. This is shown in Figure 7. Any one, two or three fuel cell loops can be effectively cooled by either or both Freon loops.

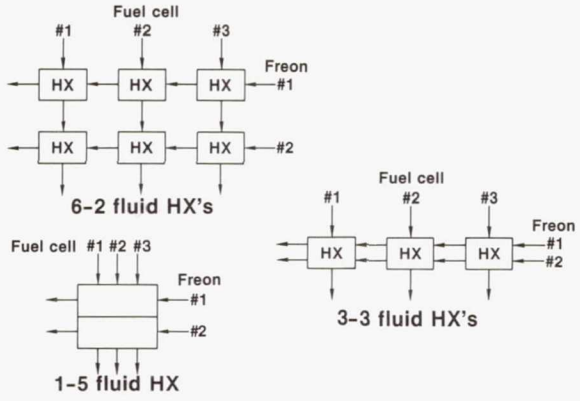

FIGURE 6 FUEL CELL HEAT EXCHANGER CANDIDATE APPROACHES

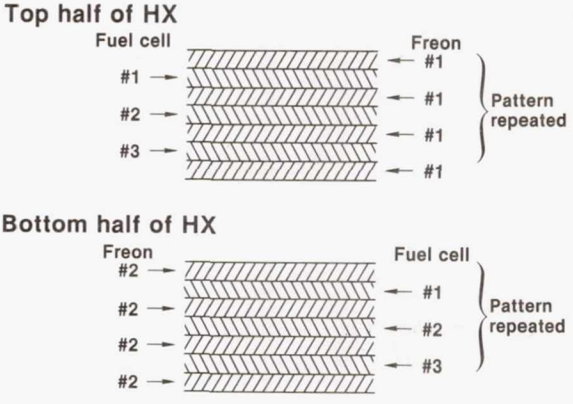

FIGURE 7 FUEL CELL HEAT EXCHANGER LAYERS

Headering

In order to achieve high performance, counterflow within the heat exchanger core is desired. When flowing four separate fluid loops through the same core efficient headering is difficult. A novel combination of internal and external headers was devised that provides counterflow through most of the core. Figure 8 presents two layers of a typical heat exchanger showing the semicircular external headers and the flow distributing internal finned headers. The triangular ends of the core are called "tent tops". One of the fluids enters the core on the end of the tent top, flows the length of the core and exits on the opposite side of the other tent top. The other fluid enters at the side of the core in the tent top area, flows the length of the core in the other direction and exits on the opposite side. As can be seen most of the core is counterflow. The internal header finned sections are well slotted to aid in flow distribution. Poor flow distribution that adversely affected thermal performance was observed during initial development testing of an Interchanger. Tolerance studies indicated that fin passages near the edge of the core could be blocked. A computer flow distribution analysis was conducted that defined the slotting required in the inlet sections to properly distribute flow. Subsequent units exhibited no maldistribution or performance deficiencies.

The final configurations for the Interchanger and fuel cell heat exchanger are shown in the photographs of Figures 9 and 10.

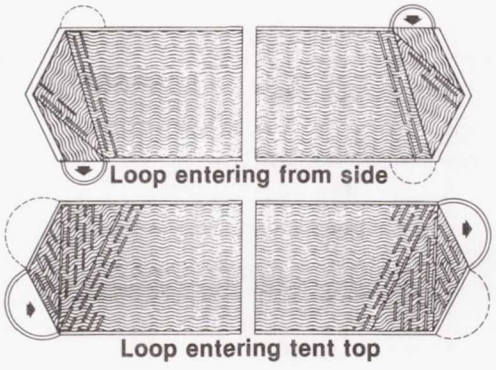

FIGURE 8 TYPICAL HEAT EXCHANGER FIN CONFIGURATION

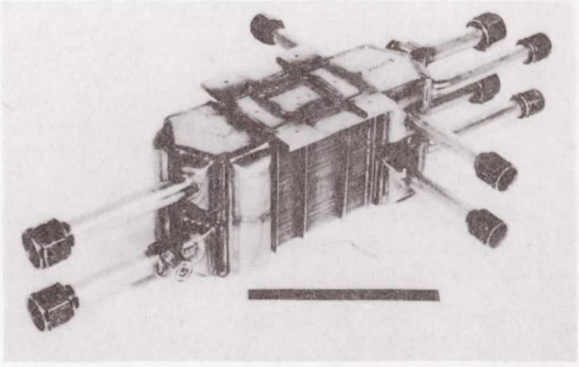

FIGURE 9 FUEL CELL HEAT EXCHANGER

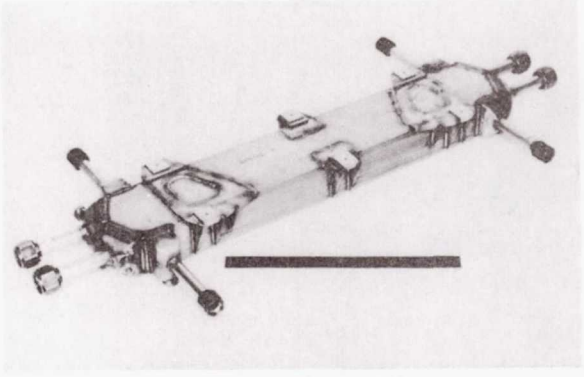

FIGURE 10 INTERCHANGER

WATER EVAPORATION

Water evaporation was selected as a heat rejection means for the following reasons:

- o Water is the best evaporant from a weight standpoint since it has the largest latent heat of vaporization of any candidate fluid. This minimizes the evaporant weight penalty for cooling required during launch and an abort following launch.
- o A large quantity of excess water is produced by the fuel cell power system. Although not nearly enough water is produced for total heat rejection during the entire mission, water is available for supplementary heat rejection on-orbit when the vehicle attitude reduces the radiator capability.
- o A water evaporator can be used to expel excess water as steam when the water storage tanks reach maximum capacity. The steam can be expelled at high velocity through a nozzle and directed away from the vehicle to reduce contamination of the environment in the immediate vicinity.

Previous spacecraft used water evaporators for heat rejection. Mercury, Gemini and the Apollo command module used wick-feed boilers and the Lunar Module, Saturn V and Apollo space suit used porous plate sublimators. All of these devices have response, heat load range and life limitations. Early in the shuttle program, NASA concluded that a new concept for water evaporation would be advantageous and the flash evaporator evolved.

Flash evaporation involves spraying water on the walls of a chamber that is heated by Freon coolant. The spray chamber is maintained at a pressure (saturation pressure) low enough for the water to evaporate at a temperature below the desired Freon outlet temperature. Since a Freon outlet temperature of 40°F maximum is required, the chamber pressure must be maintained at or below about 0.1 psia (35°F saturation temperature). In flash evaporation, it is imperative that all of the water that reaches the wall be instantly evaporated to prevent excessive carryover or flooding and eventual freezing causing failure of the device.

The low evaporation pressure is maintained on-orbit by venting the steam generated overboard to space vacuum through a sonic nozzle. As the heat load is reduced, the pressure will fall because of reduced steam flow and may drop below the triple point aggravating the potential freezing situation.

In the flight unit, water is introduced into the chamber in a pulsing manner for temperature control reasons. This causes the chamber pressure to fluctuate during each cycle with minimum pressures below the triple point. A detailed description of the Flash Evaporator Subsystem and a discussion of its flight performance are presented in Reference 2 and 3 respectively.

Because of the potential freezing problems and the dynamic nature of flash evaporation, it was necessary to perform extensive analyses and to conduct basic research on flash evaporation to thoroughly understand the process and aid in the design of the flight system.

Three typical areas of investigation concerning the design and development of the flash evaporator are detailed in the following sections:

- o The basic research program conducted at Rice University to better understand the process.
- o The analytical effort in the form of a thermal math model performed during the design and testing phases.
- o Flash evaporator and integrated ATCS testing conducted at NASA-JSC.

In addition to the above, significant effort was expended in developing the desired hollow cone water spray distribution and droplet size distribution and in analyzing the steam flow pattern and velocities within the evaporator using finite element techniques to predict water droplet carryover.

FES Description

A brief description of the flash evaporator subsystem is in order before the details of its operating characteristics are discussed. A more detailed description can be found in Reference 1 and 2.

The FES (Figure 11) contains two evaporators, three controllers (two primary and one secondary), two sets of feedwater spray valves, nine temperature sensors and thermostatically heated exhaust steam ducts. Figure 12 presents the FES schematic. Freon flows in two loops through both evaporators in series - first, through a "high load" unit, then through a "topping" unit. Both evaporators operate during launch and entry but only the "topper" operates in orbit.

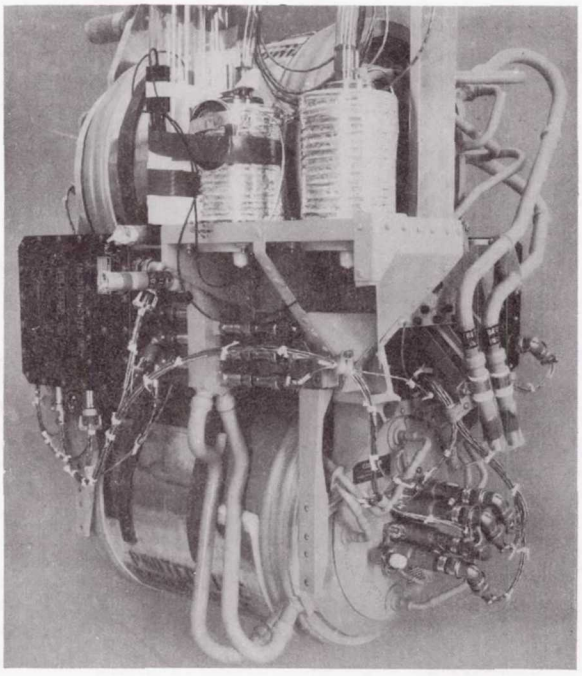

FIGURE 11 FLASH EVAPORATOR PACKAGE

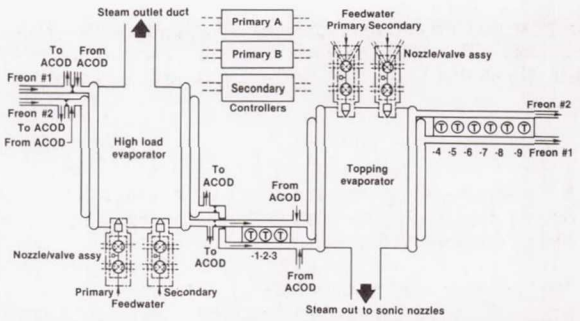

FIGURE 12 FLASH EVAPORATOR ASSEMBLY SCHEMATIC

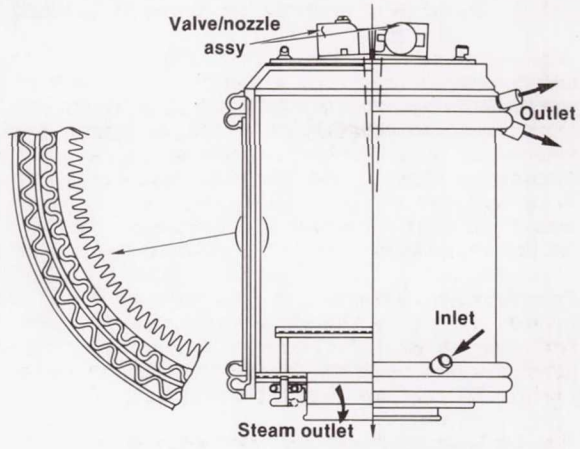

FIGURE 13 SHUTTLE EVAPORATOR

Each evaporator consists of three basic parts made of aluminum alloy: the evaporator core, the spray valve/nozzle mounting plate, and the anti-carryover device (ACOD). The cylindrical core contains the primary heat transfer surface area. At one end of the core, the valve plate provides a heated mounting surface for the spray valves. At the opposite end of the core, the anti-carryover device aids in evaporating any water carried by the steam flow before it leaves the evaporator.

In order to enhance the evaporative heat transfer area and water retention, the internal surfaces of the cores are grooved in an axial direction as shown in Figure 13. Two concentric annular finned passages carry the dual Freon loops longitudinally within each core from the anti-carryover device to the valve plate end.

Each valve/nozzle assembly contains an isolation valve, pulser valve, and spray nozzle. The spray nozzle distributes feedwater over the evaporator heat transfer surface. The pulser valve is pulsed open for 200 msec at a variable frequency to meter feedwater flow. The isolation valve provides redundant sealing of the feedwater line during quiescent periods and isolation of the feedwater following failure of a pulser.

Three temperature sensors monitor Freon midpoint temperature (between evaporators) and six monitor Freon outlet temperature. The three midpoint sensors and three of the outlet sensors are used by the control sections of the three controllers, and the remaining three outlet sensors are used by the three shutdown sections of the controllers.

Once activated, FES startup and shutoff is programmed as a function of midpoint Freon temperature. Freon outlet temperature is maintained within a band of 39 $\pm$ 1°F by one of the redundant primary controllers.

Circuitry in the secondary (abort) controller is similar to the primary controllers, except the control set point is 62 $\pm$ 2°F.

Each controller has a shutdown section physically isolated from the control section. Each shutdown section monitors the performance of the controller through a Freon outlet temperature sensor. If temperature or rate of change limits are exceeded the FES is shut down.

There are two separate steam ducts. The high load duct is relatively short (7.5 ft) with few bends. The topping duct exhausts overboard through two thrust balancing nozzles, one on each side of the vehicle. The distance from the evaporator to each nozzle is approximately 21 ft.

Basic Research Program

A spray cooling research program was initiated by Rice University, Houston, Texas, under NASA Grant NAS 9-65274. Results were reported to NASA-JSC in three separate reports during 1979 and also documented in Reference 4.

The purpose of the research, summarized in this section, was to identify the fundamental heat transfer processes involved in spray cooling, to provide experimental data useful to the design engineer, and to add to the general understanding of the overall spray cooling process. Secondarily, the effect of grooving the heat transfer surface was also evaluated.

Three distinct operating modes of spray cooling have been identified. The first is the case in which the surface vaporizes all of the impinging spray. This is called the "dry-wall" state, and the heat transfer process in this mode is called "spray evaporative cooling". The second operational mode is that in which the spray forms a thin liquid film upon the surface. This is referred to as the "flooded" state and "spray film cooling" is the name given to the associated heat transfer process. The third operational mode is that in which the liquid droplets are deflected from the surface by a thin vapor film which forms on impact. This is called the "Leidenfrost" state and heat transfer. A number of studies of these heat transfer processes has been reported in the literature. A listing of the references can be found in Reference 4.

The research conducted at Rice was primarily concerned with the dry-wall state and with the transition from it to the flooded state. The crux of the experimental investigations was determining, for spray evaporative cooling, the locus of flooding points -- that is, determining the wall temperature and corresponding heat flux at which the dry-wall to flooding transition occurs. This yields the maximum possible heat flux for each surface temperature during dry-wall operation.

The influence of various parameters upon this flooding locus was investigated. The effects of surrounding pressure, from atmospheric to just below the triple point of water were studied. The influence of a grooved surface compared to a smooth polished surface was studied. The influence of feedwater temperature and the influence of an intermittent-pulsing spray were also investigated.

The heat flux (q) during dry-wall operation is directly related to the impinging spray mass flux ($\dot{m}$). Assuming no superheating of the departing vapor

$$q = \dot{m}[\lambda + C_p(T_s - T_o)] \qquad (1)$$

where λ is the latent heat of vaporization of the spray liquid, C_p is its constant pressure specific heat, T_s is its saturation temperature, and T_o is its supply temperature. What is of interest is the wall temperature (T_w) and corresponding heat flux (q) range over which the dry-wall mode of operation may exist for a given spray mass flux.

In dry-wall operation, the wall temperature and heat flux adjust so that all the impinging spray evaporates without accumulation on the surface. If the surface temperature is lowered, with the spray unchanged, a point is reached where the droplets no longer evaporate as fast as they arrive, and liquid will begin to accumulate on the surface. This flooding point is the lower limit for spray evaporative cooling (dry-wall mode). The transition to the flooded state will be a gradual, progressive change when T_w is greater than the nucleate boiling temperature T_b of the thin liquid film. The transition is sudden, or catastrophic, when T_w is less than T_b.

Experimentally the two primary quantities to measure are the surface temperature and the heat flux through the metal surface upon which the water spray is impinging. The technique employed was to measure the axial temperature profile along an insulated aluminum cylinder heated on one end and cooled by the water spray on the other end. From this temperature profile, both the heat flux through the surface and the surface temperature were readily determined. The liquid spray was directed at the sample surface from a nozzle located above the sample; the mass rate of impingement of spray on the surface was not measurable. For a given spray mass flux, steady state operation was achieved with a temperature feedback control circuit to adjust electrical power to the heater. The entire assembly was placed in a bell jar in which the pressure was controlled by exhausting through an orifice to a liquid nitrogen cold trap by means of a vacuum pump.

Beginning with the surface in a dry-wall state, the set point to the temperature controller was lowered gradually until the surface just began to flood. At this point data was recorded. It

should be noted that "flooding" was a subjective visual determination based upon the experimenter's evaluation that the surface was just on the verge of flooding, small pools just beginning to form. For the smooth polished surface this was fairly straight forward. For the grooved surface, however, flooding was a bit more difficult to define. It was chosen as the point where some water could be standing in the grooves, but never enough to allow spanning of the grooves.

Using distilled water at 25°C sprayed from a 0.40 mm dia., 90° included angle, full-cone nozzle located approximately 45 cm above the surface, the flooding locus was determined for a smooth 6061-T6 aluminum surface at atmospheric pressure, and at average pressures of about 19, 6.76, and 4.56 mmHg. These flooding locus curves are shown in Figure 14 (data points have been eliminated for clarity).

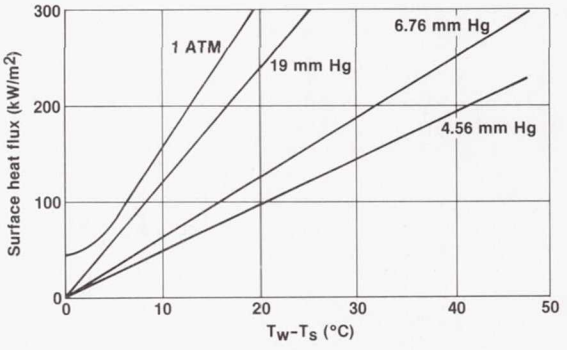

FIGURE 14 FLOODING LOCUS

For a grooved aluminum surface, the flooding locus was determined at atmospheric pressure, and average pressures of about 20.18, 7.11, and 4.51 mmHg. It was found that grooves on the surface had no apparent effect on the flooding locus or dry-wall operation. However, based on testing conducted at Hamilton Standard, grooves do improve water retention and help spread unevaporated water to less stressed areas in a flight evaporator configuration.

Knowledge of the flooding locus is particularly important for operation at pressures below the triple point of water (4.587 mmHg). At such pressures, excess water on the surface creates the potential for freezing. For both surfaces studied, at pressures below the triple point, it was observed that for values of $T_W - T_S$ less than about 15°C, freezing would begin at the interface of the heated surface and the surrounding Teflon insulation (the coolest points on the surface). The ice formation then moved rapidly inward above the surface and formed an ice cap over the entire surface. Once formed, increasing the heating rate through the surface would not stop the ice growth (the surface just got hotter). The only way to halt the growth of the ice cap was to raise the pressure to a value above the triple point. On doing so, melting began immediately. Increasing the pressure proved to be the only effective means of controlling ice formation. A procedure for doing this on the flight unit was developed during testing at NASA-JSC.

Water freezing and accumulating on poorly heated surfaces was also experienced on the flight configuration evaporator. Great care was exercised in the design of the core to assure that all areas receiving spray would be heated sufficiently to prevent ice formation.

Testing was conducted using a pulsing-intermittent rather than a steady state spray at low pressure. A nozzle with a solenoid valve was operated with a fixed "on-time" of 200 msec and an on-off pulsing frequency variable between 0 and 4 hz, thus allowing the spray "duty cycle" to be varied.Tests were run at 7.11 mmHg and at atmospheric pressure. Attempts were made to operate at pressures below the triple point, but at these low pressures the accumulation of water on the nozzle negated proper spray operation. This accumulation of water on the nozzle at very low pressures is thought to be associated with solenoid operating in the nozzle; it was not observed at pressures above the triple point or for continuous operation. A great deal of development effort was spent on the flight configuration spray valves to reduce the valve "dribble volume" and prevent valve freezing.

The results obtained suggest that with pulsing duty, the spray evaporative cooling process is not basically different from that with continuous duty. The flooding locus is the same in either case; it occurs, for a given wall temperature, at a heat flux lower than continuous duty by the ratio of the duty cycle of the pulsing spray.

A number of measurements were attempted at low pressures using feedwater at temperatures greater than 25°C. It was found that for water temperature greater than about 40°C, the water droplets leaving the nozzle "instantaneously" evaporated -- flash evaporation -- particularly in the interior of the spray. The large vapor plume so formed negated a reasonably steady spray reaching the heated surface in the apparatus used. It was concluded that for a given system operating pressure, there is an upper limit on the feedwater temperature above which the effectiveness of the spray evaporative cooling process is negated because of the spray flashing directly to vapor before reaching the surface to be cooled.

All of the flooding locus data obtained in the experiments at Rice University may be summarized, as shown in Figure 15, by defining a "flooding coefficient"

$$h^* = q^*/(T_{flood} - T_s) \qquad (2)$$

which is simply the slope of each flooding locus, and is dependent upon the operating pressure, or perhaps more conveniently the saturation temperature of the liquid spray. For the designer, the variable of interest is the wall temperature T_w rather than $(T_w - T_s)$. Figure 15 could be used to determine the best operating pressure (saturation temperature) to yield the largest attainable heat flux without flooding.

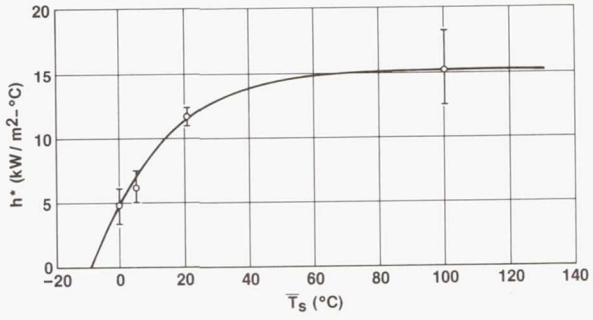

FIGURE 15 FLOODING COEFFICIENT

The linear flooding loci determined experimentally suggest that a conduction-controlled droplet evaporation model might serve as an adequate analytical model for predicting the flooding coefficient h*. Such a model was developed and documented in reports to NASA-JSC under the previously mentioned NASA grant. Agreement of the analytical results for atmospheric pressure with those obtained from experiment are close enough to give confidence in the model and suggest that further study might yield fruitful results.

FES Thermal Model

A computer model of the FES was written to study and predict its dynamic behavior. This model includes the effects of water spray distribution on the core walls, dual Freon loops at varying inlet conditions, cyclic steam pressure resulting from a pulsing water spray and steam exhaust duct flow characteristics and the control laws that modulate spray pulsing to control Freon outlet temperature. The highly dynamic nature of the FES results from the short 200 millisecond pulses of water sprayed onto the core at controlled intervals and the low thermal inertia of the evaporator. These pulses of water are rapidly evaporated upon contacting the hot core walls heated by the Freon. Steam pressure quickly builds up in the core as the water evaporates and then rapidly decays as the pulse of water spray ends and the steam exits from the duct. In the subsystem, the important dynamic parameters are the Freon temperatures, the amount of water sprayed into the core and evaporated, the steam pressure in the core, and the controller signals to modulate the short 200 millisecond pulses of water.

Freon temperatures are calculated throughout the subsystem. The evaporator itself is divided into an Anti-Carryover Device (ACOD) zone, a core wall zone, and a valve plate zone as shown in Figure 16. In the evaporator core wall zone where the temperature distribution is crucial to determine the amount of water evaporation, as fine a division of the core wall into segments as desired can be made. Figure 17 shows one of these segments as used in the computer model. Any loss of heat from the Freon to the core wall results in a decrease in Freon temperature; this is modeled for each Freon segment by applying the First Law of Thermodyanmics as follows:

$$M_f(i)C_{pf}\frac{d\bar{T}_f(i)}{dt} = \dot{m}_f C_{pf}[T_{fin}(i)-T_{fout}(i)]-h_f A(i)[\bar{T}_f(i)-T_w(i)] \qquad (3)$$

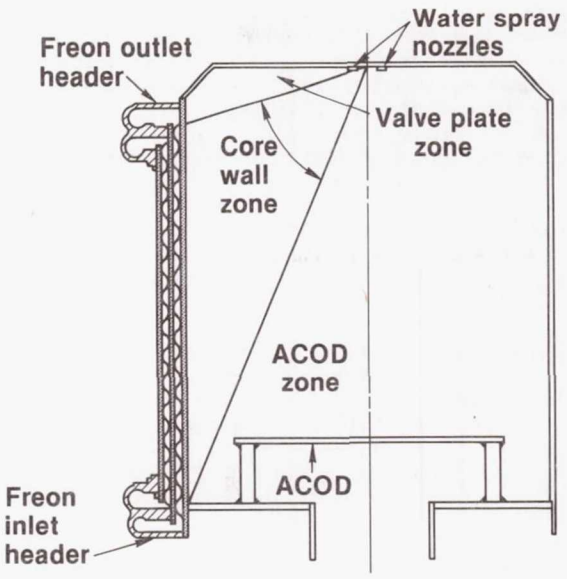

FIGURE 16 SPRAY ZONES

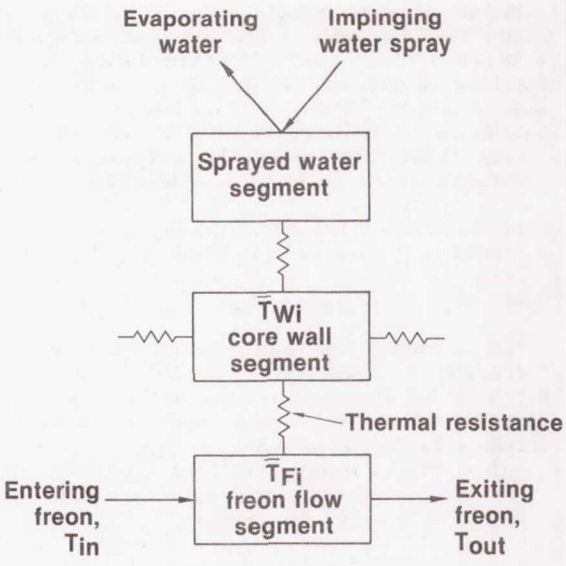

FIGURE 17 THERMAL MODEL

A similar energy balance is applied to the evaporator core wall whereby its temperature changes whenever an unbalance exists between the heat input from the Freon and the heat loss to the impinging water spray:

$$M_w(i)C_{pw}\frac{dT_w(i)}{dt} = C[T_w(i-1)-T_w(i)]-C[T_w(i)-T_w(i+1)]-Q_e(i)+h_f A(i)[\bar{T}_f(i)-T_w(i)] \quad (4)$$

The thermodynamics and heat transfer on the water spray is the most dynamic and the most challenging to model. The water leaving the nozzle impinges on the various zones and segments of the core in different amounts. This distribution varies with feedwater temperature and pressure and is different for the high load and topping evaporators. A spray distribution factor was defined and correlated to test data to arrive at the following expression which gives the general shape of all spray distributions:

$$f(\beta) = 0.5\{1 + \tanh[m(\beta - \phi)]\} \quad (5)$$

The factors ϕ and m are functions of feedwater temperature and pressure. A typical cumulative spray distribution is shown in Figure 18.

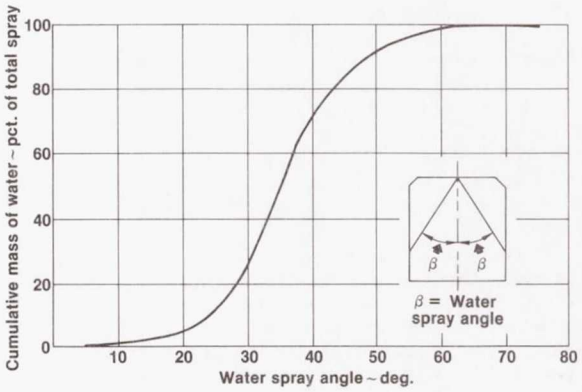

FIGURE 18 SPRAY DISTRIBUTION

The water impinging on a segment of the core is then evaporated at a rate dependent upon the difference in temperature between the wall and the temperature of the steam in the core. The temperature of the steam is at the saturation temperature corresponding to the pressure in the core. As the steam evaporates, the pressure and therefore the temperature rises in the core until the spray stops. Then, the pressure and temperature decrease as the steam exits the core. Steam pressure is a function of the flow characteristics of the exhaust duct system. Depending on the rate of evaporation, all the water impinging on the core may not evaporate before the beginning of the next spray pulse. The division of the core into segments permits the calculation of the precise spot where this buildup of water may occur. Division of the core into fewer segments would average over this spot and would not predict any water buildup when there actually may be one. This highly dynamic rising and falling of the steam temperature and pressure is therefore coupled in the model with the spray and wall temperature distributions to determine the amount of impinging spray that is evaporated in the core and thereby the heat removed from the Freon.

The pulsing of the spray is regulated by the controller to cool the freon to an outlet temperature of 39^{0}F. To model the controller, the actual electronic circuitry was analyzed. As in the controller, the computer model translates the incoming temperatures into voltages and applies the control laws. The control includes a combination of proportional, integral and differential gains with lead-lag compensation. When the control law output voltage reaches six volts, a 200 millisecond spray pulse is initiated; and the control law output voltage is reset to zero. In addition to the control laws, the shutdown logic and the control laws for the secondary controller are included in the computer model.

Modelling the Flash Evaporator Subsystem on a digital computer presented a major technical challenge. More than twenty simultaneous partial differential equations with time constants sometimes orders of magnitude different had to be solved. The Gear Method,[5] which is a multistep predictor corrector method whose order and time increments are automatically chosen as the integration proceeds, was used effectively to produce computer running times as low as 1/3 of real time.

In spite of the inherent difficulty in modelling the highly dynamic FES, the computer program has been used successfully to predict test data, to establish acceptance criteria for controller operation, and to simulate ground test and flight operation.

FES Testing

The FES presented a performance verification challenge. Because of the size of the steam exhaust ducting, the actual flight configuration could not be tested at a commercial facility. FES performance testing was conducted using a duct simulator. The simulator consisted of a short duct section, a large diameter volume and adjustable exit orifice. The large volume was necessary to simulate the volume of the flight duct configuration. The orifice was adjusted to give the same steady state evaporator pressure as the flight configuration when operated in the Hamilton Standard chamber. Chamber pressure could not be maintained at space vacuum levels and reached 1 mmHg at maximum steam flow.

In order to fully qualify the FES for flight, it was deemed necessary to test the flight configuration under expected flight conditions. Two series of tests were conducted in the Space Environmental Simulation Laboratory (SESL) at NASA-JSC. It was necessary to use the large chamber A for these tests.

The first series of tests (OFEST) was conducted with a flight configuration FES as the only test hardware. Testing included:

- o Simulated launch and entry ambient pressure transients.
- o Simulated Freon inlet temperature transients.
- o Steady state performance limits.
- o Testing to help size the orifice in the duct simulator used at Hamilton Standard.
- o Steam exhaust plume evaluation.

The second series of tests (Integrated ATCS Tests) was conducted with a flight configuration FES plus additional ATCS hardware, including a space radiator panel, in an integrated system test. Testing included:

- o Actual system transient performance
- o Evaluation of failure conditions
- o Radiator panel performance

A major accomplishment of the testing relative to the FES was the establishment of a cleanout or thawing procedure in the unlikely event of a freeze-up on-orbit. Following the intentional flood-

ing of the evaporator, the secondary controller that controls Freon outlet temperature to 62°F was used to raise the evaporator steam pressure above the triple point. Under these conditions, thawing of ice accumulated in the core occurred quite rapidly and completely.

CONCLUSIONS

The major ATCS challenges were met using a combination of established system engineering techniques, basic research, sophisticated analytical techniques and extraordinary testing. In the process, advances in the state-of-the-art of heat exchanger design and manufacture were effected. These advances resulted in significant weight and particularly volume reductions over what were previously typical spacecraft heat exchanger configurations. In order to realize these gains, it was necessary to perform extensive system level optimization trade-off studies, extrapolate existing sizing techniques to much denser fin configurations and develop improved manufacturing techniques. All of the heat exchangers in the ATCS met or exceeded predicted performance during ground test and flight.

Flash evaporation at pressures below the triple point had never been attempted previously in spacecraft heat rejection. In fact, it was not a well understood process. A system, based on basic flash evaporation research and extensive analytical modeling, was developed that met all of the high response, high heat load range and long life requirements of the orbiter. The FES also can be considered an advance in the state-of-the-art in spacecraft expendable heat rejection. During the development process, basic knowledge of the spray evaporation process and how to control it was gained. With the exception of some minor temperature sensor anomalies on the first two shuttle flights, the FES has performed flawlessly.

REFERENCES

(1) Trusch, R. B., Nason, J. R., "Compact Heat Exchangers for the Space Shuttle", 75-ENAs-54, American Society of Mechanical Engineers publication, presented at the 5th Intersociety Conference on Environmental Systems, San Francisco, California, July 21-24, 1975.

(2) Nason, J. R., Decrisantis, A. A., "Shuttle Orbiter Flash Evaporator", 79-ENAs-14, American Soceity of Mechanical Engineers publication, presented at the 9th Intersociety Conference on Environmental Systems, San Francisco, California, July 16-19, 1979.

(3) Nason, J. R., Behrend, A. F., Jr., "Shuttle Orbiter Flash Evaporator Operational Flight Test Performance", 820883, Society of Automotive Engineers publication, presented at the 12th Intersociety Conference on Environmental Systems, San Diego, California, July 19-21, 1982.

(4) Grissom, W. M., Wierum, F. A., "Spray Cooling of a Heated Surface", published in the International Journal of Heat and Mass Transfer, Vol. 24, pp. 261-271, 1981.

(5) Gear, C. W., "DIFSUB for Solution of Ordinary Differential Equations", published in the Communications of the ACM, March 1974, Vol. 14, Number 3.